Subsurface Cracks Under Conditions of Slip, Stick, and Separation Caused by a Moving Compressive Load

S. D. Sheppard
Department of Mechanical Engineering,
Stanford University,
Stanford, CA 94305

J. R. Barber

M. Comninou
Department of Mechanical Engineering and
Applied Mechanics,
University of Michigan,
Ann Arbor, MI 48109

The Mode I and II stress intensity factors (K_I, K_{II}) *at the two tips of a subsurface crack subjected to a moving compressive load are studied. Coulomb friction along the crack faces results in a number of history dependent slip-stick configurations and nonsymmetric variation in* K_I *and* K_{II}. *The formulation used to study this variation involves a singular integral equation in two variables which must be solved numerically, and because of the history dependence, requires an incremental solution. Crack lengths and coefficients of friction that result in as many as three zones for any load location are considered in this paper, while a previous paper (Sheppard et al., in press) was limited to configurations involving two zones only.*

Introduction

The geometry shown in Fig. 1 depicts a subsurface crack that might lead to a spalling failure in a component experiencing rolling contact (e.g., roller and ball bearing, wheel and rail, cam and follower). P in this figure represents the load transferred from one component to another.

Experimental evidence (Ramanathan and Radhakriskhnan, 1977; Jahanmir and Suh, 1977) shows that the subsurface crack may grow parallel to the surface for some distance, after which a transverse crack forms, ultimately leading to detachment of a thin layer of material. Fatigue mechanisms are present in this growth. Additional evidence (Yoshimura et al., 1984) has shown that crack growth is greater from crack tip C (trailing crack tip) than from crack tip B (leading crack tip). This asymmetric behavior, (which may initially seem in conflict with the fully reversed shear stress predicted in Hertzian contact between elastic bodies) can be explained either by plastic deformation or by the presence of friction between the crack faces. The effect of crack face friction and the resulting history dependence are considered in this paper.

By assuming linear elastic fracture mechanics (LEFM), very small crack growth per load pass, and Coulomb crack face friction, Sheppard et al. (in press) studied the range of the Mode II stress intensity factors (ΔK_{II}) for cracks embedded in an elastic half-space, as shown in Fig. 1, subjected to a moving compressive surface load. Dimension a represents the crack depth, t the monotonically increasing load position, and B and

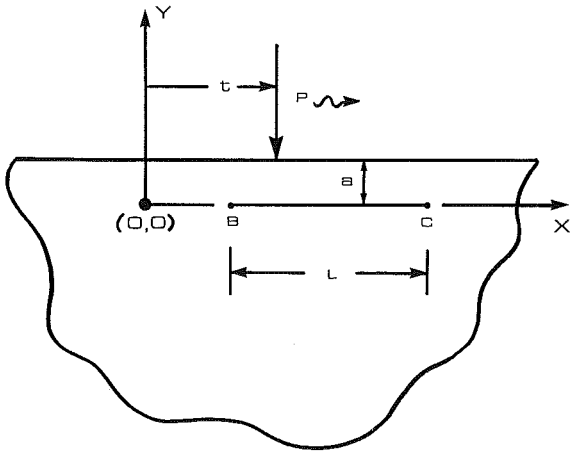

Fig. 1 Geometry of the problem

C the extent of the crack of length L. They found that as the load moves from left to right (slowly enough for inertia effects to be negligible), a number of stick-slip configurations develop, each of which is dependent on the previous load history, the crack length to depth ratio L/a, and the coefficient of crackface friction f. Because several of these configurations involve a growing stick zone, the problem had to be solved incrementally for reasons discussed in the work by Sheppard et al. (in press).

It was found that except for very short cracks (e.g., $f=0.10$, $L/a=0.10$), ΔK_{II} at C is greater than ΔK_{II} at B, which is consistent with the observed crack growth by Yoshimura et al. (1986). The investigation by Sheppard et al. (in press) was restricted to combinations of f and L/a that follow a pattern such that no configuration develops that consists of more than 2 zones. These combinations are referred to as "Short Cracks."

The present paper extends the formulation developed by

Contributed by the Applied Mechanics Division for presentation at the 1987 Applied Mechanics, Biomechanics, and Fluids Engineering Conference, Cincinnati, OH, June 14–17, 1987, of the American Society of Mechanical Engineers.
Discussion of this paper should be addressed to the Editorial Department, ASME, United Engineering Center, 345 East 47th Street, New York, N.Y. 10017, and will be accepted until two months after final publication of the paper itself in the JOURNAL OF APPLIED MECHANICS. Manuscript received by ASME Applied Mechanics Division, June 20, 1985; final revision, July 20, 1986.
Paper No. 87-APM-29.

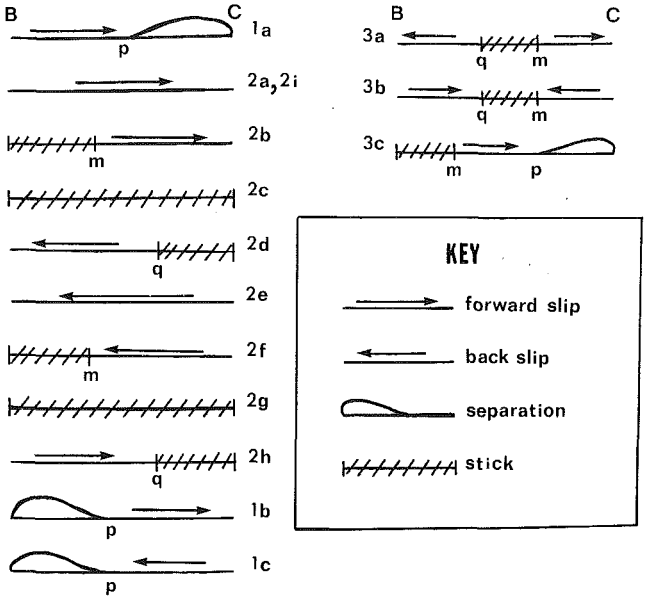

Fig. 2 Configurations investigated in the current work and in the work by Sheppard et al. (in press)

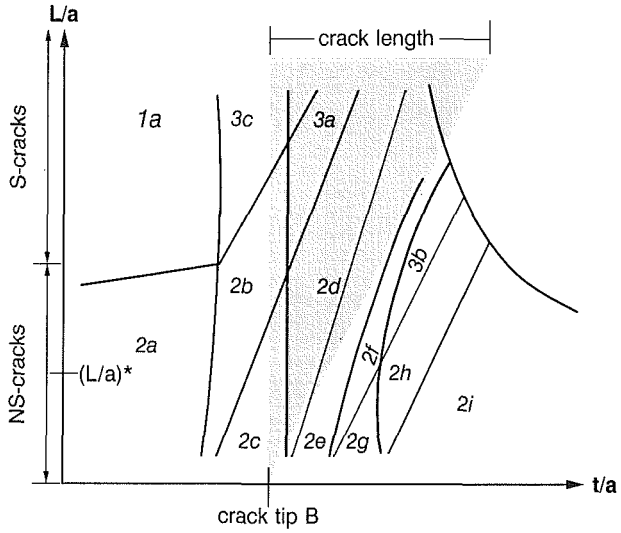

Fig. 3 Generic configuration map. Development of configurations with left to right load movement for a specific value of L/a.

Sheppard et al. (in press) to consider combinations that result in configurations where more than 2 zones and/or separation occur at some load location. The assumptions of LEFM, Coulomb crack face friction, and slow crack growth are retained, as is the geometry of Fig. 1. Of particular interest is the influence f and L/a on the range of stress intensity factors experienced at crack tips B and C.

Details of the analysis that are similar to those presented by Sheppard et al. (in press) are not repeated here.

The Semi-Inverse Method

One of four conditions can exist between the upper and lower crack faces, namely, forward slip, back slip, stick, or separation. Each condition is governed by two equalities and one or two inequalities. Furthermore, all portions of the crack are *not* necessarily under the same condition at a given load condition.

The pattern of configurations (i.e., the way in which different combinations of stick, slip and/or separation develop with load movement) is not known a priori. This necessitates that the solution be approached in a semi-inverse manner, i.e., a configuration for a particular load position is assumed and the resulting tractions are found using the governing equalities. The governing inequalities are then checked. If they are not violated, the assumed configuration is correct. If they are, the sense of the violation gives an indication of the true configuration for this load position, and the problem must be resolved with a new assumed configuration. In this manner, it is possible to determine what configurations develop with load movement, even though this is not known a priori.

The Configuration Map

As was mentioned previously, the investigation by Sheppard et al. (in press) was restricted to cracks of (L/a) such that only one and two zone configurations developed with load movement, as represented by configurations $(2a)$–$(2i)$ of Fig. 2. This particular situation develops only with cracks of (L/a) less than a critical value $(L/a)^*$, which is a function of the coefficient of friction f.

The transitions between configurations can be plotted as a function of load position and L/a, to give a configuration map, as shown in Fig. 3. This figure shows the development of configurations for a range of L/a ratios (vertical axis) with load movement (horizontal axis) for a particular coefficient of friction. It is read by selecting a specific level of L/a, then traversing the plot along a horizontal line at that level, noting that crossing a boundary line indicates a change in the configuration. At $L/a > (L/a)^*$, configurations involving 3-zones and/or separation develop in addition to those represented by $(2a)$–$(2i)$ presented by Sheppard et al. (in press). The results represented in this map must be interpreted from left to right because of the history dependent nature of the problem.

It is the objective of this current paper to explore crack patterns developed at $L/a > (L/a)^*$. The formulation of configurations $(2a)$–$(2i)$ is contained in the work by Sheppard et al. (in press), while that for additional configurations that develop at $L/a > (L/a)^*$ is presented below and in the work by Sheppard (1985). All of the configurations investigated by Sheppard et al. (in press) and in the present work are summarized in Fig. 2.

Formulation

The problem is formulated by using the solution for a compressive load on an unflawed half-plane, corrected by additional solutions which ensure that appropriate boundary conditions are met along the crack. The unflawed half-plane shear and normal tractions are given by the Flamant Solution, as was discussed by Sheppard et al. (in press).

One of the two corrective terms is represented by a distribution of edge dislocations of the glide type with density $B_x(x)$. This distribution depends on the position of the load, t, but the dependence is only indicated explicitly when needed for clarity. The shear and normal tractions associated with the glide dislocation distribution are given by the seconds terms in both equations (3) and (4) of the work by Sheppard et al. (in press), respectively, where K_s is replaced with K_{sg}, and K_n with K_{ng} in the current presentation. In the following development equations contained in the work by Sheppard et al. (in press) will be referred to by $\{xx\}$.

The second corrective term, which is only needed when separation is present, is represented by a distribution of edge dislocations of the climb type with density B_y along the separation zone. As with the B_x distribution, B_y depends on the position of the load, t, but the dependence is only indicated explicitly when needed for clarity. The shear and normal tractions associated with this climb dislocation distribution are (Schmueser et al., 1980):

$$S_c(x) = \frac{2\mu}{\pi(k+1)} \int_B^C B_y(\xi) K_{sc}(x,\xi) d\xi \qquad (1)$$

$$N_c(x)=\frac{2\mu}{\pi(k+1)}\int_B^C B_y(\xi)K_{nc}(x,\xi)d\xi \tag{2}$$

where

$$K_{sc}(x,\xi)=\frac{8a^3}{R^2}\left(3-\frac{16a^2}{R}\right) \tag{3}$$

$$K_{nc}(x,\xi)=\frac{1}{(x-\xi)}-\frac{(x-\xi)}{R}\left(-1+\frac{4a^3}{R}+\frac{64a^4}{R^2}\right) \tag{4}$$

and $R=4a^4+(\xi-x)^2$.

Combining the Flamant, glide, and climb terms for shear and normal tractions results in

$$S(x)=\frac{2Pa^2x_t}{\pi(a^2+x_t^2)^2}+\frac{2\mu}{\pi(k+1)}\int_B^C B_x(\xi)K_{sg}(x,\xi)d\xi$$

$$+\frac{2\mu}{\pi(k+1)}\int_B^C B_y(\xi)K_{sc}(x,\xi)d\xi \tag{5}$$

$$N(x)=\frac{-2Pa^3}{(a^2+x_t^2)^2}+\frac{2\mu}{\pi(k+1)}\int_B^C B_x(\xi)K_{ng}(x,\xi)d\xi$$

$$+\frac{2\mu}{\pi(k+1)}\int_B^C B_y(\xi)K_{nc}(x,\xi)d\xi \tag{6}$$

The Mode II stress intensity factors K_{II} at B and C are given in equations {5} and {6} and the horizontal shift $h(x)$ in {7} and {8}.

The Mode I stress intensity factors at B and C are

$$K_I(B)=-\lim_{x\to B}\left[\frac{2\mu}{\pi(k+1)}B_y(x)\sqrt{2\pi(x-B)}\right] \tag{7}$$

$$K_I(C)=\lim_{x\to C}\left[\frac{2\mu}{\pi(k+1)}B_y(x)\sqrt{2\pi(C-x)}\right] \tag{8}$$

We note that K_I is only nonzero if there is a separation zone adjacent to the crack tip. The vertical movement of the upper crack face relative to the lower face (i.e., gap) is

$$g(x)=v(x,0+)-v(x,0-) \tag{9}$$

and is related to $B_y(x)$ by

$$g(x)=-\int_B^x B_y(\xi)d\xi \tag{10}$$

To ensure uniqueness of displacements the integral of the dislocation distributions along the crack must be zero, i.e.,

$$\int_B^C B_y(\xi)d\xi=0 \tag{11}$$

The corresponding condition on B_x is equation {9}.

We assume that Coulomb friction exists between contacting crack faces, governed by the equations and inequalities shown below.

Forward slip:

$$S(x)=-fN(x);\quad g(x)=0 \tag{12a}$$

$$N(x)<0;\ \dot{h}(x)>0 \tag{12b}$$

Backslip:

$$S(x)=fN(x);\quad g(x)=0 \tag{13a}$$

$$N(x)<0;\ \dot{h}(x)<0 \tag{13b}$$

Stick:

$$\dot{h}(x)=0;\ g(x)=0 \tag{14a}$$

$$S(x)<-fN(x);\ N(x)<0 \tag{14b}$$

Separation:

$$S(x)=0;\ N(x)=0 \tag{15a}$$

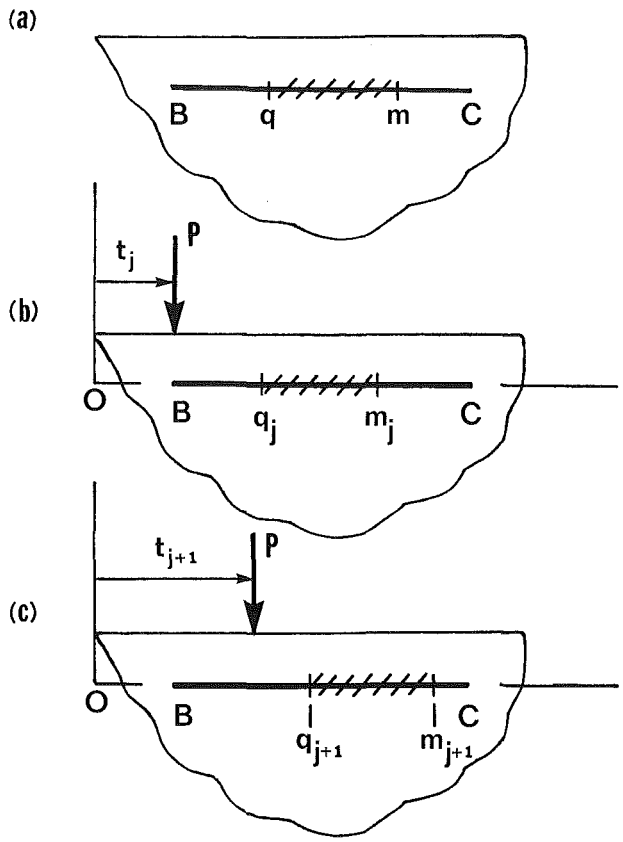

Fig. 4 3-zone configuration (3a): (a) general configuration; (b) configuration at $t=t_j$; (c) at $t=t_{j+1}$

$$g(x)>0 \tag{15b}$$

where $\dot{h}(x)=dh(x)/dt$.

For example, if a point R is a forward slip region, the expressions for N and S from equations (5) and (6) are substituted into the first equality of equation (12a) giving

$$\frac{2\pi}{\pi(k+1)}\int_B^C B_x(\xi)[K_{sg}(x,\xi)+fK_{ng}(x,\xi)]d\xi$$

$$+\frac{2\mu}{\pi(k+1)}\int_B^C B_y(\xi)[K_{sc}(x,\xi)+fK_{nc}(x,\xi)]d\xi \tag{16}$$

$$=\frac{2Pa^2(fa-x_t)}{(a^2+x_t^2)^2}\ \text{in}\ R$$

The second equality in equation (12a) requires

$$B_y(\xi)=0; \tag{17}$$

outside the separation zone.

(1a) Forward Slip with Separation. The configuration which involves a growing forward slip zone and separation is shown by (1a) in Fig. 2. It is described by equation (12) enforced over the range $B<x<C$, and the second equation of (15a) enforced over $p<x<C$ where $B<p<C$.

For some cracks a violation to the second inequality of (12b) is found just to the right of B before p has reached C. This indicates that stick begins at B. The configuration discussed in Section (3c) of stick, forward slip and separation then becomes appropriate. If p reaches C and no violation is found, a configuration of full forward slip develops, and Section 2(a) of the work by Sheppard et al. (in press) is appropriate.

(1b) Separation and Forward Slip. As the load moves to the right all combinations of f and L/a develop into a configuration of separation and forward slip, called (1b). This

configuration is basically the same as that presented in (1*a*) except that separation will extend over a region $B<x<p$, and forward slip over $p<x<C$. A Mode I stress intensity factor will develop at crack tip B, as given by equation (7), but was generally found to be small.

(1*c*) Separation and Backslip. For certain combinations of f and L/a, a configuration of separation and backslip develops after configuration (2*e*) of full backslip. The formulation for this separation-backslip configuration is identical to that of (1*b*) except that the direction of slip is reversed by substituting $-f$ for f in the relevant equations.

(3*a*) Backslip-Stick-Forward Slip. If a violation to the condition that $|S|<-fN$ occurs at B during configuration (2*b*) of growing stick and forward slip, the development of a backslip zone at B is indicated. When this occurs we must deal with configuration (3*a*), which is detailed in Fig. 4(*a*). A growing backslip zone exists in $B<x<q$ which observes condition (13), a shrinking forward slip zone exists in $m<x<C$, which observes condition (12), and a moving stick zone exists in $q<x<m$, which follows condition (14). The left zone is similar to the growing backslip zone of Section (2*d*) of the work by Sheppard et al. (in press) which did not require an incremental solution, while the right zone is similar to the growing stick zone as discussed in section (2*b*) of that same work, which did require an incremental solution. Using these ideas, the movement of q, the transition point between backslip and stick, and m, the transition point between stick and forward slip with load position, can be studied.

The shear and normal tractions at t are represented by equation (5) and (6), noting that the terms involving climb dislocations B_y are zero because there is no separation along the length of the crack. Substituting these into the first equality of (12*a*), used to describe the right zone, resuls in equation (16). Differentiating equation (16) with respect to load position, as was done in Section (2*b*) of the paper by Sheppard et al. (in press), results in an expression in which only the currently active dislocations are present:

$$\frac{2\mu}{\pi(k+1)}\int_m^C \dot{B}_x(\xi)[K_{sg}(x,\xi)+fK_{ng}(x,\xi)]d\xi$$
$$=\frac{-2\mu}{\pi(k+1)}\int_B^q \Delta\dot{B}_x(\xi)[K_{sg}(x,\xi)+fK_{ng}(x,\xi)]d\xi$$
$$+\frac{2Pa^2(4fax_t-3xt^2+a^2)}{\pi(a^2+x_t^2)^2};\quad m<x<C \tag{18}$$

The first term to the right of the equality sign represents the effect of the distribution of active dislocations in the left backslip zone on the differential problem, and, therefore, a coupling of the left and right zones. In the problem presented in Section (2*b*) of the paper by Sheppard et al. (in press) this term was zero as there was no backslip zone to account for.

Equation {23} is appropriate for partially enforcing uniqueness. Normalizing and discretizing equations (18) and (23) results in $(n+1)$ equations for finding the normalized values of $\dot{B}_x$ at specified integration points, and current load position t_{j+1}, if the transition point m_{j+1} between stick and forward slip, as shown in Fig. 4(*c*), is assumed known. The contribution from the coupling term (i.e., $\Delta\dot{B}_x$) is calculated from load position t_j, as will be discussed below.

We now turn our attention to the left slip zone where backslip is occurring. We start by writing equations (5) and (6), expressions for normal and shear tractions, in a modified form, where t_{j+1} and m_{j+1} refer to the current locations of load and stick-forward slip transition, and t_j and m_j refer to the previous locations of these points, as shown in Figs. 4(*b*) and 4(*c*).

$$S(x)=\left[\frac{2\mu}{\pi(k+1)}\int_B^q \Delta B_x(\xi)K_{sg}(x,\xi)d\xi+S_d(x)\right.$$
$$\left.+\frac{2\mu}{\pi(k+1)}\int_{t_j}^{t_{j+1}}\int_{m(z)}^C \dot{B}_x(\xi)K_{sg}(x,\xi)d\xi dz\right]$$
$$+\frac{2Pa^2x_t}{\pi(a^2+x_t^2)^2} \tag{19}$$

$$N(x)=\left[\frac{2\mu}{\pi(k+1)}\int_B^q \Delta B_x(\xi)K_{ng}(x,\xi)d\xi+N_d(x)\right.$$
$$\left.+\frac{2\mu}{\pi(k+1)}\int_{t_j}^{t_{j+1}}\int_{m(z)}^C \dot{B}_x(\xi)K_{ng}(x,\xi)d\xi dz\right]$$
$$-\frac{2Pa^3}{(a^2+x_t^2)^2} \tag{20}$$

where $x_t=x-t_{j+1}$. The bracketed term in each of these expressions represents the total effect of dislocations from the load location when stick just began at B, up to and including the present load location t_{j+1}, and is equivalent to the non-Flamant portions of equations (5) and (6). It is instructive to review what each of the parts of the bracketed terms in equations (19) and (20) represents. The first component represents the effect of the glide dislocations positioned in $B<\xi<q$, reflecting load movement from its position when backslip just begins at B up to t_{j+1}, the second component represents contributions from locked dislocations with load movement from the start of stick at B to t_j, and the final component reflects the effect from locked dislocations from local movement t_j to t_{j+1}. Substituting equations (19) and (20) into the first equality of equation (13*a*) and rearranging results in

$$\frac{2\mu}{\pi(k+1)}\int_B^q \Delta B_x(\xi)[K_{sg}(x,\xi)-fK_{ng}(x,\xi)]d\xi$$
$$=\frac{-2\mu}{\pi(k+1)}\int_{t_j}^{t_{j+1}}\int_{m(z)}^C \dot{B}_x(\xi)[K_{sg}(x,\xi)$$
$$-fK_{ng}(x,\xi)]d\xi-\frac{2Pa^2(fa+x_t)}{\pi(a^2+x_t^2)^2}+fN_d(x)-S_d(x);$$
$$B<x<q \tag{21}$$

Note that the range of equation (21) coincides with the limits of integration and that ΔB_x is bounded at q and unbounded at B. $\dot{B}_x$ is represented as in equation {24}. Uniqueness of the solution is enforced by

$$\int_B^q \Delta B_x(\xi)=0 \tag{22}$$

Normalizing equations (21) and (22), then discretizing, results in $(n+1)$ equations for finding the n values of $\Delta B_x(r)$ at specified integration points and the location of q_{j+1}, based on the value of t_{j+1} found from the solution of equations (18) and {23}, as was discussed above.

The change in the Mode II stress intensity factor at B is given by equation {43}, while that at C is given by {37}. Updates to "tracer" point stresses due to locked-in dislocations are made in the same manner as in Section (2*b*) of the work by Sheppard et al. (in press) (e.g., equation {35}).

As m moves towards C the value of forward slip dh/dt is continually monitored in the two slip zones. If it becomes positive adjacent to B the growth of a stick zone emanating from B is indicated and the problem will involve 4 zones. If the normal stress just to the right of B becomes positive, separation at this location is indicated. If separation or stick at B is not indicated, the $(j+2)$th step in the incremental solution is taken; namely finding t_{j+2} and q_{j+2} corresponding to m_{j+2}.

Before beginning calculations for this step, the left backslip

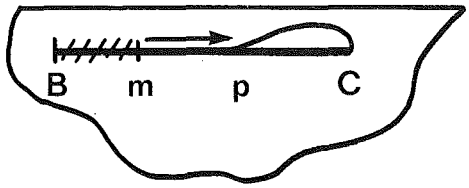

Fig. 5 3-zone configuration (3c) of stick-forward slip-separation

zone is viewed in an incremental manner at the $(j+1)$th step. This is done so that an accurate estimate can be made of first term to the right of the equality sign in equation (18) involving $\Delta\dot{B}_x(\xi)$, as was mentioned above. Equation (21) is differentiated with respect to t, and as $\Delta\dot{B}_x(\xi)$, $B<\xi<q_{j+1}$, is unbounded at both ends, provides $(n-1)$ equation is normalized, discretized form. A uniqueness requirement on $\Delta\dot{B}_x$ provides the nth equation necessary for finding $\Delta\dot{B}_x$. The accuracy of this estimate is based on the fact that load steps are small.

If a 4-zone configuration does not develop as m moves towards and finally reaches C, the problem once again becomes 2-zone in nature, following the growing backslip development of Section (2*d*) in the work by Sheppard et al. (in press).

(3*b*) Forward Slip-Stick-Backslip. In the event that configuration (3*b*) develops, as shown in Fig. 2, the formulation to be used is identical to that described in Section (3*a*) except for a change in the sign of f in appropriate equations.

(3*c*) Stick-Forward Slip-Separation. If the separation zone at end C does not disappear prior to an indication of stick at B, configuration (3*c*) develops, which is detailed in Fig. 5. Condition (12) describes the zone from $m<x<C$, while equation (15) describes $p<x<C$, and equation (14) describes $B<x<m$. This configuration differs from (1*a*) where separation was also present because the growing stick zone makes the configuration incremental in nature. The formulation used to investigate this configuration is similar to that of (2*b*), except that a distribution of climb dislocations must be included to account for the separation zone, and is detailed in the work by Sheppard (1985).

Results

Using the formulations described above and in the work by Sheppard et al. (in press), configuration maps for a number of realistic values of f were developed, an example of which is given in Fig. 6 for $f=0.5$. Note that as L/a approaches zero the results indicate that only one zone will be present at any load position.

The range of L/a ratios studied by Sheppard et al. (in press) (i.e., "Short Cracks") are indicated in this figure. "A" pattern cracks, which occur at slightly larger values of L/a than for "Short Cracks" experience a 3-zone configuration (3*b*) after the configuration of full backslip (2*e*), while "B" pattern cracks experience 3 zone configurations after full backslip (2*e*) as well as after full forward slip (2*a*). "C" pattern cracks are such that the separation zone to the left of crack tip C has not disappeared prior to the onset of stick at crack tip B (3*c*), but separation does disappear prior to an indication of backslip at B. Finally, "D" pattern cracks are such that separation has not disappeared prior to the indication of backslip at B.

It is interesting to note that for $f=0.5$ and $2.35<L/a<2.5$ configuration (1*c*) of separation and backslip develops after full backslip (2*e*). At a later load position a violation to the requirement that $(dh/dt<0)$ is found just to the left of C, indicating formation of a stick zone at this location. For $2.50<L/a<3.0$, separation develops at B during configuration (3*a*) of backslip, stick, and forward slip, and for $1.4<L/a<2.35$ during configuration (3*b*) of forward slip, stick and backslip, or (2*h*) of forward slip and stick.

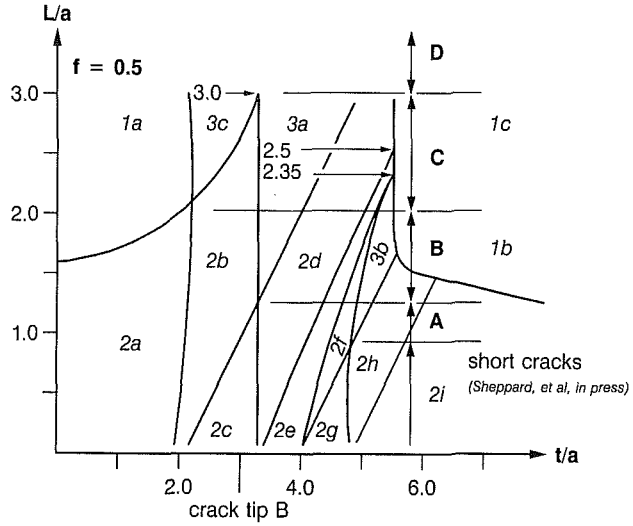

Fig. 6 Configuration map for $f=0.50$, showing configuration development for a variety of L/a values with load movement t/a

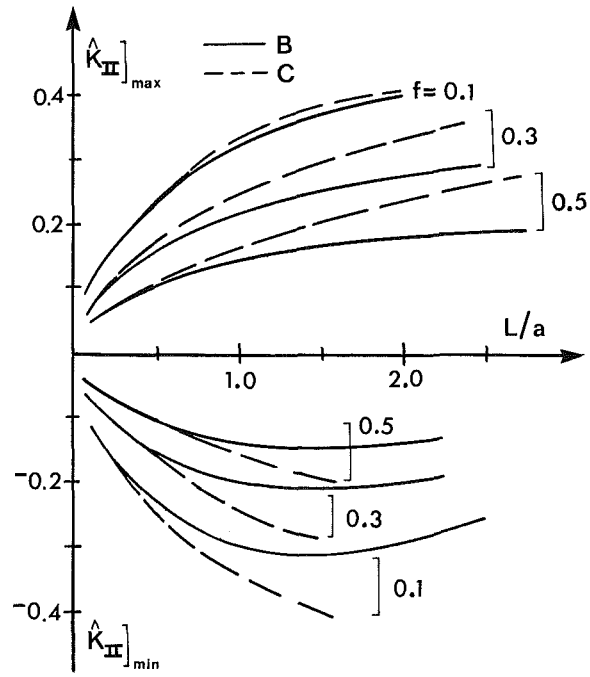

Fig. 7 Maximum and minimum values of Mode II stress intensity factors at B and C as functions of crack length L/a for various coefficients of friction

The maximum and minimum values of $\hat{K}_{II}=(\pi a^{1/2}/2P)K_{II}$ are shown in Fig. 7 as a function of crack length for various coefficients of friction. For a given L/a ratio, these values represent the maximum and minimum level of Mode II stress intensity experienced at the leading (end B) and trailing (end C) crack tips as the load moves over the crack. For all values of f considered, $\hat{K}_{IImin}(B)$ peaks at approximately $L/a=1.5$, then increases. $\hat{K}_{IImax}(C)$ appears to be leveling off in all cases. Increasing f serves to decrease all peak values.

The values of $\hat{K}_{Imax}(C)$ as a function of L/a are shown in Fig. 8 for a variety of f levels. This maximum occurs during configuration (1*a*), and similar values were found for $\hat{K}_{Imax}(B)$, which will of course occur sometime after separation has begun at B. Note how *small* these values are relative to the $\hat{K}_{II}$ values shown in Fig. 7.

Of particular importance for crack growth is the range of the stress intensity factors at the crack tips. Figure 9 shows this

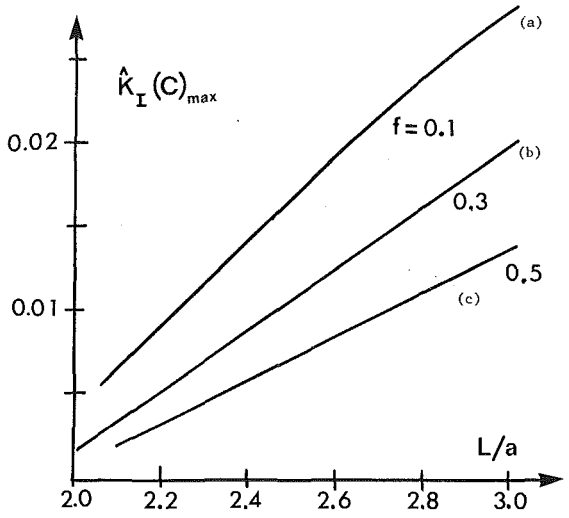

Fig. 8 Maximum values of Mode I stress intensity factors at *C* as a function of crack length *L/a* for various coefficients of friction

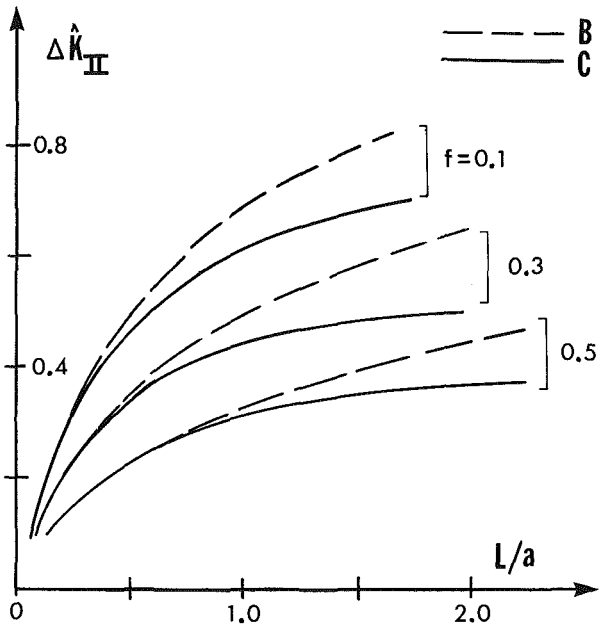

Fig. 9 The range ($\hat{K}_{IImax} - \hat{K}_{IImin}$) of Mode II stress intensity factors at *B* and *C* as functions of crack length *L/a* for various coefficients of friction

range for $\hat{K}_{II}$ as a function of L/a for various values of f. Except for very short cracks, this range is significantly greater at C than at B, indicating a tendency for cracks to grow from the trailing edge under repeated loading.

$\Delta\hat{K}_{II}$ values found in this study are compared with those presented by Hearle and Johnson (1984, 1985) in Fig. 10. At longer lengths, Hearle and Johnson's underestimation of $\Delta\hat{K}_{II}$ values is probably due to their use of an inexact model of the locked regions of the crack, and to a lesser degree due to their neglect of the influence of the free surface and crack face separation.

Conclusions

The method described allows for investigation of both Mode I (K_I) and Mode II (K_{II}) effects experienced by a subsurface crack as a load moves over the surface, as might represent fatigue in rolling contact. This method accurately reflects the history dependent nature of the problem caused by the presence of crack face friction.

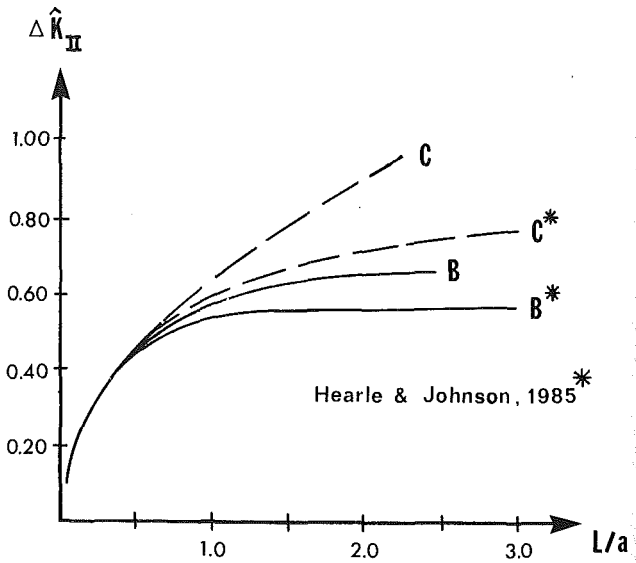

Fig. 10 Comparison of the maximum range of Mode II stress intensity factors ($\Delta\hat{K}_{II}$) with the approximate solution of Hearle and Johnson (1984, 1985): $f = 0.50$

It was found that a number of configuration patterns will result, depending upon the combination of L/a and f. However, these patterns are all such that the crack is left in a stress free state when the load is far away. The parallel nature of a number of the lines separating configurations, as shown in Fig. 6, leads us to anticipate that there is some limiting pattern which is experienced by all cracks beyond a certain length.

In all cases investigated, it was found that $\Delta K_{II}(C)$ is greater than or equal to $\Delta K_{II}(B)$, being equal only when L/a is small. This finding is consistent with the experimental evidence presented in by Yoshimura et al. (1984). As L/a increases, $\Delta K_{II}(B)$ and $\Delta K_{II}(C)$ appear to level off.

The Mode I stress intensity factors at both B and C are at least an order of magnitude smaller than K_{II}, and therefore most likely do not affect crack growth significantly. The presence of Mode I action must be included in the model however, in order to accurately describe interaction between the upper and lower crack faces. Increasing friction serves to decrease all stress intensity factors.

Acknowledgment

Support by the Office of Naval Research through the contract N00014-K-0287 during the course of this research is gratefully acknowledged.

References

Hearle, A. D., Johnson, K. L., 1985. "Mode II Stress Intensity Factors for a Crack Parallel to the Surface of an Elastic Half-Space Subjected to a Moving Point-Load," *J. Mech. Phys. Solids*, Vol. 33, No. 1, pp. 61-81.

Hearle, A. D., Johnson, K. L., "Mode II Stress Intensity Factors for a Crack Parallel to the Surface of an Elastic Half-Space Subjected to a Moving Point-Load," C-Mech/TR26, Cambridge University Engineering Department.

Jahanmir, S., Suh, N. P., 1977. "An Overview of the Delamination Theory of Wear," *Wear*, Vol. 45, pp. 1-16.

Ramanathan, V. M., Radhakrishnan, V. M., 1977. "Investigation of Rolling Contact Fatigue Damage in Case-Carburized Low Alloy Steel," *Wear*, Vol. 45, pp. 323-333.

Schmueser, D., Comninou, M., Dundurs, J., 1980. "Separation and Slip Between a Substrate Caused by a Tensile Load," *Int. J. Engng. Sci.*, Vol. 18, pp. 1149-1155.

Sheppard, S. D., 1985. "Subsurface Cracks in Rolling Contact," Ph.D. Thesis, University of Michigan, Mechanical Engineering.

Sheppard, S., Barber, J. R., Comninou, M., in press. "Short Subsurface Cracks Under Conditions of Slip and Stick Caused by a Moving Compressive Load," *J. of Appl. Mech.*

Yoshimura, H., Rubin, C. A., Hahn, G. T., 1984. "Cyclic Crack Growth Under Repeated Rolling Contact," *Wear*, Vol. 95, p. 29.